American Mineralogist, Volume 86, pages 981–989, 2001

Temperature-dependent single-crystal neutron diffraction study of natural chondrodite and clinohumites

ALEXANDRA FRIEDRICH,[1,*] GEORGE A. LAGER,[2] MARTIN KUNZ,[1] BRYAN C. CHAKOUMAKOS,[3] JOSEPH R. SMYTH,[4] AND ARTHUR J. SCHULTZ[5]

[1]Laboratorium für Kristallographie, ETH Zentrum, Sonneggstrasse 5, CH-8092 Zürich, Switzerland
[2]Department of Geography and Geosciences, University of Louisville, Louisville, Kentucky 40292-0001, U.S.A.
[3]Solid State Division, Oak Ridge National Laboratory, Oak Ridge, Tennessee 37831-6393, U.S.A.
[4]Department of Geological Sciences, University of Colorado, Boulder, Colorado 80309, U.S.A.
[5]Intense Pulsed Neutron Source Division, Argonne National Laboratory, Argonne, Illinois 60439-4814, U.S.A.

ABSTRACT

The crystal structures of natural F-bearing chondrodite [$Mg_{4.64}Fe_{0.28}Mn_{0.014}Ti_{0.023}(Si_{1.01}O_4)_2F_{1.02}OH_{0.97}$] from the Tilley Foster mine (Brewster, New York), F-bearing titanian clinohumite [$Mg_{8.805}Fe_{0.006}Ti_{0.214}(Si_{0.993}O_4)_4F_{0.484}OH_{0.516}$] from Kukh-i-Lal (Tadjikistan) and F-free titanian hydroxylclinohumite [$Mg_{7.378}Fe_{1.12}Mn_{0.052}Ni_{0.014}Ti_{0.453}(Si_{0.996}O_4)_4OH_{1.0}$] from Val Malenco (Italy) were refined in space group $P2_1/b$ (unique axis *a*) from single-crystal neutron diffraction data, collected on a four-circle diffractometer at the High Flux Isotope Reactor at Oak Ridge National Laboratory. Accurate H atom positions were determined at 295 K, 100 K, and 20 (10) K. Only one H position of approximately 50% occupancy was observed for each structure, which confirms a disordered H model. Time-of-flight single-crystal neutron data were also collected at 295 K and 20 K for the Val Malenco clinohumite as an additional check on space group symmetry. The crystal structure of the Kukh-i-Lal clinohumite was further investigated by X-ray single-crystal refinement at 295 K and by piezoelectric measurements. A few, very weak, symmetry-forbidden reflections were observed for each crystal at both ambient and lower temperatures. The same reflections were observed by all methods used. No temperature dependence is indicated, as no additional peaks appear at low temperature, and the intensity of the reflections are sample dependent. It appears that the real structure is made up of $P2_1$ and *Pb* domains so that violations are due to ordering of both H and Ti. No distinct piezoelectric effect was observed that would indicate the absence of a center of symmetry. This points to the simultaneous presence of various enantiomorphic domains, which cancels the piezoelectric effect of individual domains. The decrease in unit-cell volume with F substitution in clinohumites can be explained by the higher concentration of H-site vacancies and the coupled cationic and anionic substitution on the M3 and O/F site.

INTRODUCTION

Early fundamental studies of the structures of the humite group minerals [$nM_2SiO_4 \cdot M_{1-x}Ti_x(F,OH)_{2-2x}O_{2x}$, where M is Mg with minor amounts of Fe^{2+}, Mn, Ni, Ca, Zn, Cu, $0 < x < 0.5$], their nomenclature and chemical composition were carried out by Gibbs, Ribbe, and co-workers (Gibbs and Ribbe 1969; Jones 1969; Jones et al. 1969; Ribbe et al. 1968; Ribbe and Gibbs 1971). These authors focused on norbergite ($n = 1$), chondrodite ($n = 2$) and humite ($n = 3$). This series was continued by single-crystal structure refinements of clinohumite ($n = 4$) and titanian clinohumite (Robinson et al. 1973; Kocman and Rucklidge 1973; Fujino and Takéuchi 1978), and hydroxylchondrodite (Yamamoto 1977), as well as by the comprehensive work by Ribbe (1979; 1982) on the whole humite series. Recently, the H position of norbergite (Cámara 1997), and the two H positions of naturally occurring hydroxylclinohumite (Ferraris et al. 2000) were determined by single-crystal X-ray diffraction methods. The O-D···O bond geometry in both deuterated hydroxylchondrodite and deuterated hydroxylclinohumite has been examined using neutron powder diffraction methods (Lager et al. 2001; Berry and James 2001). The humite minerals are a homologous series of magnesium orthosilicates whose structures are based on slightly distorted hexagonal close-packed (hcp) arrays of anions (O, F, OH) with one-half of the octahedral sites occupied by M and 8–12% of the tetrahedral sites occupied by Si (Ribbe 1982). The non-standard monoclinic space group $P2_1/b$ (unique axis *a*) for chondrodite and clinohumite is used in order to emphasize the structural relationship to olivine. The *a* crystallographic axis is chosen parallel to the 6_3 axis of an ideal hcp anion array. In terms of a polyhedral model the dominant structural units are chains of edge-sharing octahedra, running parallel to the *c* axis and cross-linked by SiO_4 tetrahedra. The asymmetric unit of the chondrodite structure has three octahedrally coordinated M

* E-mail: alexandra@kristall.erdw.ethz.ch

sites, one tetrahedrally coordinated Si site, five oxygen positions and one H position; the clinohumite structure has five M sites, two Si sites, eight oxygen positions, and one H position (Fig. 1). The (F, O, OH) anion is triangularly bonded to three M cations, one M2, and two M3. End-members hydroxylchondrodite (Yamamoto 1977; Lager et al. 2001) and hydroxylclinohumite (Ferraris et al. 2000; Berry and James 2001) have two symmetrically different H sites occupied. Yamamoto (1977) included the positions of the H atoms for synthetic hydroxylchondrodite as refineable parameters in the least-squares analysis, and proposed positional disorder for the protons. A statistical distribution of the OH orientation among the equilibrium positions satisfies the symmetry conditions of the space group $P2_1/b$ and explains the elongated displacement parameter ellipsoid of the O atom, which serves as both acceptor and donor. This disordered model has been recently confirmed by Lager et al. (2001). Fujino and Takéuchi (1978) have located the centrosymmetrically related, partially occupied H sites in a titanian clinohumite from difference-Fourier maps. In nature only Ti-rich chondrodite and clinohumite are F-free among humite group minerals. Both Ti-free hydroxylchondrodite and hydroxylclinohumite have been synthesized at high pressures and temperatures (Yamamoto and Akimoto 1977; Akaogi and Akimoto 1980).

There is renewed interest in chondrodite and clinohumite because they may be constituents of the Earth's lower crust and upper mantle, and therefore could provide a means of storage for water in this region. The close structural relationship to olivine, a major constituent of the upper mantle, and the structurally bound H make them interesting materials for creating models for the incorporation of water in olivine and the mechanisms of transport of water into the Earth's upper mantle (Thompson 1992).

For the above reasons, several papers have been published that deal with chondrodites and clinohumites in the past ten years. Spectroscopic data have been used to extract elastic properties (Fritzel and Bass 1997; Sinogeikin and Bass 1999) and the pressure and/or temperature dependence of OH vibrational frequencies (Williams 1992; Lin et al. 1999; Mernagh et al. 1999; Lin et al. 2000). The influence of the $F(OH)_{-1}$ substitution on the H-atom environment has also been investigated by spectroscopic methods (Akaogi and Akimoto 1986; Cynn et al. 1996; Phillips et al. 1997). Diffraction data have been used to study the effect of the OH/F ratio on the compressional behavior. Bulk moduli have been reported for F-bearing chondrodite (Faust and Knittle 1994; Kuribayashi et al. 1998; Friedrich et al. 2000) and for hydroxylchondrodite and hydroxylclinohumite (Ross and Crichton 2000; Lager et al. 1999).

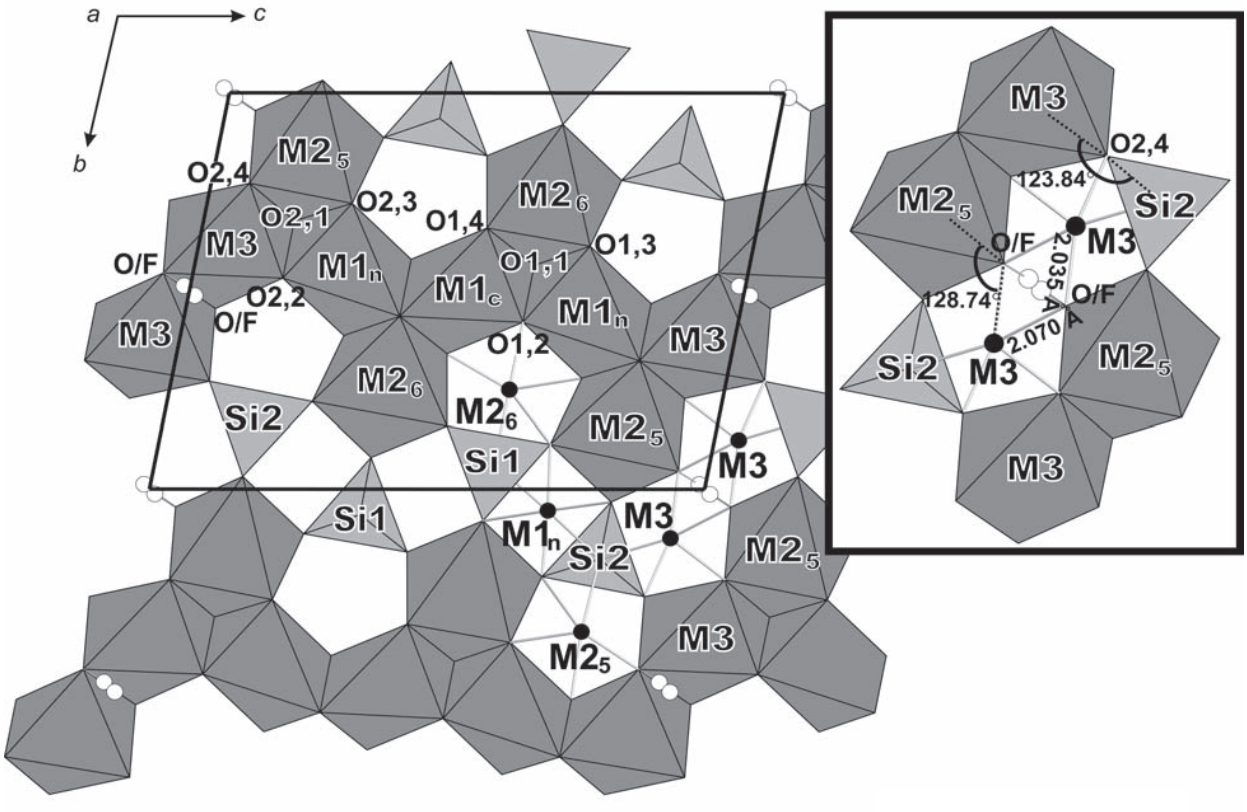

FIGURE 1. The crystal structure of clinohumite projected on the (100) plane with bond distances from the Val Malenco sample. Open circles represent H sites; filled circles M sites. The inset highlights the symmetrically distinct bonds and angles around the O/F site (see also text). The O/F atoms associated with the two labeled M3-O/F bonds are located in the polyhedral sheet below the one illustrated, i.e., the O/F-O/F edge is not shared between M3 octahedra. Distances are given in angstroms.

In this work, a neutron single-crystal diffraction study was undertaken to determine accurate hydrogen positions of naturally occurring F-free titanian-hydroxylclinohumite, F-bearing clinohumite and F-bearing chondrodite. The goal of this study is to present data on the structural environment of H in chemically diverse (OH/F ratio) natural humites at both ambient and lower temperatures.

Experimental methods

Titanian hydroxylclinohumite from Val Malenco (Italy) occurs as megacrysts in ultramafic serpentinite veins (Weiss 1997). The quality of an opaque, dark red-brown crystal was checked with several X-ray photographs produced by the Laue back-scattering technique to exclude twinning and domains. A $3.7 \times 4.0 \times 3.0$ mm crystal was cut from the sample for the neutron experiment. The specimen from Kukh-i-Lal (Pamir, Tadjikistan) is a light orange-yellow, F-bearing gem-quality titanian clinohumite from marbles. The F-bearing chondrodite sample from Tilley Foster mine (Brewster, New York) was obtained from the Smithsonian Museum (no. C3200-10). It is a transparent, orange-brown crystal that was cut into a prism of approximate dimensions $1.50 \times 2.35 \times 3.60$ mm. The chemical composition of the chondrodite (8 analyses) and clinohumite (22 analyses) samples was determined using a Cameca SX 50 electron microprobe (EMA) (15 kV, 20 nA, 5 µm electron beam diameter) (Table 1). Standards used were forsterite (Mg, Si), rutile (Ti), corundum (Al), chromite (Cr), fayalite (Fe), tephroite and rhodonite (Mn), NiO (Ni), and F-rich phlogopite (F). For the F-analysis a PC1 analyzer multi-layer crystal with a 2d-value of ~60 Å was used. Data collection time was 20 s. Peak-background ratio was used to determine elemental concentrations. The OH^- content was calculated from stoichiometric constraints based on 13 and 7 cations, respectively.

Neutron single-crystal diffraction data were collected at 295, 100, and 20 K (10 K for the chondrodite) on the HB2a four-circle diffractometer at the high-flux isotope reactor (HFIR) at Oak Ridge National Laboratory (ORNL). A wavelength of 1.0037(2) Å was obtained using a (331)Ge monochromator at a take-off angle of 45°. The crystals were glued to an aluminium pin and mounted on the cold-tip of a closed-cycle He refrigerator, which is mounted on the diffractometer for low-temperature measurements. A set of 31 to 40 reflections for the clinohumites and 72 to 102 reflections for chondrodite were used for refining the unit-cell parameters (Table 2) and determining the orientation matrix. Intensity-data collection was carried out by radially scanning through the Ewald sphere. At the limits of $2\theta = 0°$ and 180° the radial scan is a pure ω scan and a pure θ-2θ scan, respectively. A simple trigonometric relationship controls the relative speeds of the ω and 2θ motors at intermediate values. A 1/4-sphere of Bragg reflections was measured to $\sin\theta/\lambda = 0.763$ Å^{-1}. Three reflections were monitored to correct the intensities for variations in the neutron flux, which did not change by more than 1% for the duration of each data collection. The intensities were integrated using the Lehman-Larsen algorithm and corrected for the Lorentz effect with the UCLA Crystallographic Computing Package (1994, personal communication). The intensities of equivalent monoclinic reflections were then averaged, giving approximately 2750 reflections for each data set. Due to shadowing effects caused by the mounting brackets of the refrigerator, reflections at angles in a range of about $2\theta > 100°$ and $92° \le 2\theta \le 100°$ with $-77° \le \chi \le -61°$ were excluded from refinements. Details on the data collection are summarized in Table 3.

The structures were refined in the space group $P2_1/b$ (unique axis *a*) using the General Structure Analysis System (GSAS), (Larson and Von Dreele 1994). Starting values in the refinements for chondrodite and clinohumite were those reported by Gibbs et al. (1970) and Robinson et al. (1973, ICSD no. 4569), respectively. The initial values for the H positions for

Table 1. Electron microprobe analyses of the samples of this work. Unit formulae calculated on the basis of 18 (clinohumite) and 10 (chondrodite) O atoms (Ribbe 1982)

	Val Malenco	Kukh-i-Lal	Tilley Foster
		wt% oxides	
SiO_2	35.6(3)	37.8(2)	34.7(8)
TiO_2	5.4(2)	2.71(7)	0.5(1)
Al_2O_3	0.004(6)	0.01(1)	0.009(8)
Cr_2O_3	0.011(1)	0.01(1)	0.01(1)
FeO	11.9(2)	0.07(2)	5.7(7)
MnO	0.55(3)	0.02(2)	0.28(4)
NiO	0.16(4)	0.014(15)	0.02(2)
MgO	44.3(3)	56.3 (3)	53.5(8)
F	0	2.30(7)	5.5(8)
H_2O*	1.47(4)	1.17(2)	2.5(4)
O=F	0	–0.97(3)	–2.3(3)
Total	99.4(5)	99.5(4)	100.4(7)
		unit formulae	
Si	3.98(2)	3.97(1)	2.02(4)
Ti	0.45(1)	0.214(5)	0.023(6)
Al	0.0005(8)	0.001(1)	0.0005(5)
Cr	0.0010(9)	0.0009(9)	0.0003(4)
Fe^{2+}	1.1(2)	0.006(2)	0.28(4)
Mn	0.052(2)	0.001(1)	0.014(2)
Ni	0.014(4)	0.001(1)	0.0008(7)
Mg	7.38(2)	8.81(2)	4.64(7)
F	0	0.76(2)	1.0(2)
H	1.10(3)	0.82(2)	1.0 (2)
*X**			
X_{Fe}	0.131(2)	0.0007(2)	0.056(2)
X_{Ti}	0.45(1)	0.214(5)	0.023(6)
X_F	0	0.48(1)	0.52(1)
X_{Cl}	0	0	0
X_{OH}	1.00(0)	0.52(1)	0.48(1)

* Calculated on the basis of 13 (clinohumite) and 7 (chondrodite) cations.

Table 2. Unit-cell parameters and volumes of chondrodite and clinohumites studied

	Val Malenco clinohumite			Kukh-i-Lal clinohumite			Tilley Foster chondrodite		
	295 K	100 K	20 K	295 K	100 K	20 K	295 K	100 K	10 K
a (Å)	4.7344(9)	4.7282(9)	4.7313(9)	4.7404(4)	4.7366(5)	4.7362(5)	4.7401(3)	4.7345(2)	4.7321(3)
b (Å)	10.286(1)	10.273(1)	10.274(1)	10.2380(9)	10.226(1)	10.226(1)	10.2843(7)	10.2674(5)	10.2641(5)
c (Å)	13.713(2)	13.702(2)	13.695(1)	13.651(1)	13.636(2)	13.635(1)	7.8831(5)	7.8716(3)	7.8673(4)
α (°)	101.042(8)	101.004(9)	101.029(8)	100.909(8)	100.904(9)	100.904(8)	109.097(2)	109.060(2)	109.052(2)
V (Å^3)	655.5(2)	653.3(2)	653.4(2)	650.5(1)	648.5(1)	648.4(1)	363.14(4)	361.67(3)	361.19(3)

TABLE 3. Details on data reduction and results of the temperature-dependent structure refinements

	clinohumite Val Malenco*			clinohumite Kukh-i-Lal†			chondrodite Tilley Foster‡		
	RT	100 K	20 K	RT	100 K	20 K	RT	100 K	10 K
Total $\|F\|$	2791	2746	2742	2765	2756	2755	1576	1570	1567
Averaged $\|F\|$	2448	2438	2263	2419	2410	2409	1425	1419	1416
$\|F\|_{obs}$ ($F > 3\sigma$)	1707	1647	1627	1723	1710	1704	1225	1222	1260
variables	158	158	158	153	153	153	91	91	91
χ^2	2.769	3.026	2.755	2.234	2.622	2.624	2.150	2.547	3.326
R ($F > 3\sigma$)	0.0446	0.0495	0.0468	0.0357	0.0388	0.0386	0.0326	0.0342	0.0375
Rw (Fo)	0.057	0.063	0.059	0.049	0.053	0.053	0.042	0.044	0.048
Scan rate (°/min)	2	3	3	2.5	3	3	2.5	2.5	2
Peaks for OM	40	39	39	36	36	31	102	75	71
ρ (g/cm^3)	3.280	3.291	3.280	3.202	3.219	3.218	3.162	3.172	3.178
μ (cm^{-1})	0.140			0.130			0.220		
Extinction coeff.	2.062×10^{-6}	1.641×10^{-6}	1.569×10^{-6}	8.467×10^{-5}	2.541×10^{-4}	2.531×10^{-4}	1.095×10^{-4}	1.207×10^{-4}	2.830×10^{-4}

Notes:
$\chi^2 = \Sigma\, w(F_o - SF_c)^2 / (N_{obs} - N_{var})$, w = weights, S = scale factor.
$R = \Sigma|F_o - SF_c|/\Sigma\,|F_o|$.
$Rw = [\Sigma\, w(F_o - SF_c)^2 / \Sigma\, w|F_o|]^{1/2}$.
* *hkl* range = $0 \le h \le 6$, $-15 \le k \le 15$, $0 \le l \le 20$.
† *hkl* range = $0 \le h \le 7$, $-15 \le k \le 15$, $0 \le l \le 20$.
‡ *hkl* range = $0 \le h \le 7$, $-15 \le k \le 14$, $0 \le l \le 12$.

chondrodite and clinohumite were taken from Yamamoto (1977) and Fujino and Takéuchi (1978). A Becker-Coppens Type II extinction correction was applied to each data set of the clinohumites. A Type I correction was used to characterize the extinction in chondrodite (Table 3). The Mg:Fe-ratio was refined for all M sites with the constraint that the sum of the occupancies of Mg and Fe was fixed. The EMA-derived Ti-concentration was assigned to the M3 position for the Val Malenco clinohumite, as suggested by Fujino and Takéuchi (1978). Ti occupation was thus refined for all M sites only for the Kukh-i-Lal clinohumite. The refined OH/F ratio for chondrodite shows good agreement with EMA results both in refinements with and without constraints [$\sum$(OH + F) = 1]. In the case of the Kukh-i-Lal clinohumite, the F, O, and H site occupancies were each refined independently, revealing a higher O than H occupancy. The presence of an oxy component is in agreement with the higher Ti content in this sample. The O:F ratio [with $\sum$(O + F) = 1] is equivalent to the EMA results within uncertainties. The occupancies and displacement parameters of O, F, and H were refined alternately due to their mutual dependence. The lower H content is consistent with a coupled F $\leftrightarrow$ Ti-substitution. All atom positions were refined with anisotropic displacement parameters. A numerical absorption correction was applied in the case of the Val Malenco titanian hydroxylclinohumite. The complex shape of the Kukh-i-Lal clinohumite allowed only a spherical absorption correction. The final discrepancy factors are summarized in Table 3.

Atomic parameters and isotropic displacement factors are given in Tables 4–6, site occupancies in Table 7. Selected interatomic distances and angles are presented in Tables 8 and 9 and anisotropic displacement factors in Table 10[1].

The observation of a few very weak, symmetry-forbidden reflections led us to further investigations. The space-group symmetry of the Val Malenco titanian clinohumite was also examined at 295 and at 20 K using the single-crystal, time-of-

[1]For a copy of Table 10, document item AM-01-069, contact the Business Office of the Mineralogical Society of America (see inside front cover of recent issue) for price information. Deposit items may also be available on the American Mineralogist web site (http://www.minsocam.org or current web address).

TABLE 4. Atom positions and atom displacement parameters of the Val Malenco titanian clinohumite

	RT				100 K				20 K			
	x	*y*	*z*	U_{eq}	*x*	*y*	*z*	U_{eq}	*x*	*y*	*z*	U_{eq}
$M1_c$	1/2	0	1/2	0.0077	1/2	0	1/2	0.0047	0.5	0.0	0.5	0.0044
$M1_n$	0.4965(3)	0.9459(1)	0.27458(9)	0.0080	0.4961(4)	0.9458(2)	0.2747(1)	0.0053	0.4966(4)	0.9457(2)	0.2747(1)	0.0045
$M2_5$	0.0137(3)	0.1399(1)	0.16997(9)	0.0078	0.0139(4)	0.1400(1)	0.1699(1)	0.0052	0.0145(3)	0.1403(1)	0.1700(1)	0.0046
$M2_6$	0.5103(3)	0.2504(1)	0.38774(9)	0.0078	0.5097(4)	0.2501(2)	0.3880(1)	0.0055	0.5095(4)	0.2495(1)	0.3879(1)	0.0044
M3	0.4894(4)	0.8763(2)	0.0436(1)	0.0066	0.4890(5)	0.8766(2)	0.0436(2)	0.0040	0.4890(5)	0.8766(2)	0.0437(2)	0.0035
Si1	0.0730(4)	0.0666(2)	0.3899(1)	0.0062	0.0736(5)	0.0673(2)	0.3900(2)	0.0049	0.0736(4)	0.0670(2)	0.3900(1)	0.0046
Si2	0.0757(4)	0.1765(2)	0.8349(1)	0.0063	0.0760(5)	0.1764(2)	0.8351(2)	0.0048	0.0751(4)	0.1765(2)	0.8351(1)	0.0043
O1,1	0.7332(3)	0.0644(1)	0.3883(1)	0.0082	0.7322(4)	0.0645(2)	0.3882(1)	0.0057	0.7323(4)	0.0643(2)	0.3882(1)	0.0054
O1,2	0.2805(3)	0.4204(1)	0.38773(9)	0.0073	0.2801(4)	0.4203(2)	0.3879(1)	0.0063	0.2806(3)	0.4202(1)	0.3880(1)	0.0053
O1,3	0.2220(3)	0.1129(1)	0.29424(9)	0.0080	0.2224(4)	0.1126(2)	0.2941(1)	0.0061	0.2221(3)	0.1127(2)	0.2941(1)	0.0061
O1,4	0.2205(3)	0.1588(1)	0.48682(9)	0.0083	0.2212(4)	0.1585(2)	0.4866(1)	0.0060	0.2212(4)	0.1588(2)	0.4866(1)	0.0055
O2,1	0.2355(3)	0.3233(1)	0.16345(9)	0.0078	0.2352(4)	0.3237(2)	0.1634(1)	0.0064	0.2350(4)	0.3234(1)	0.1633(1)	0.0055
O2,2	0.7774(3)	0.9680(1)	0.16351(9)	0.0082	0.7769(4)	0.9683(2)	0.1632(1)	0.0061	0.7768(3)	0.9688(2)	0.1633(1)	0.0057
O2,3	0.7234(3)	0.2792(1)	0.2614(1)	0.0087	0.7233(4)	0.2791(2)	0.2616(1)	0.0064	0.7236(4)	0.2792(2)	0.2615(1)	0.0058
O2,4	0.7245(3)	0.2285(1)	0.0692(1)	0.0090	0.7256(4)	0.2281(2)	0.0691(1)	0.0068	0.7253(4)	0.2286(2)	0.0690(1)	0.0063
O/F	0.2569(4)	0.0448(2)	0.0534(1)	0.0133	0.2562(5)	0.0450(2)	0.0534(1)	0.0108	0.2563(4)	0.0450(2)	0.0534(1)	0.0107
H	0.081(1)	0.0124(6)	0.0115(4)	0.0207	0.082(2)	0.0114(7)	0.0110(5)	0.0196	0.083(2)	0.0126(7)	0.0114(5)	0.0188

Note: Here O/F ≡ O(H), no F.

TABLE 5. Atom positions and atom displacement parameters of the Kukh-i-Lal clinohumite

	RT				100 K				20 K			
	x	*y*	*z*	U_{eq}	*x*	*y*	*z*	U_{eq}	*x*	*y*	*z*	U_{eq}
$M1_c$	1/2	0	1/2	0.0059	1/2	0	1/2	0.0033	1/2	0	1/2	0.0031
$M1_n$	0.4973(3)	0.9463(1)	0.27416(8)	0.0059	0.4971(3)	0.9462(1)	0.27420(9)	0.0031	0.4974(3)	0.9463(1)	0.27424(9)	0.0032
$M2_5$	0.0109(3)	0.1401(1)	0.16985(8)	0.0061	0.0107(3)	0.1403(1)	0.16975(9)	0.0036	0.0108(3)	0.1403(1)	0.16970(9)	0.0035
$M2_6$	0.5085(3)	0.2502(1)	0.38824(8)	0.0058	0.5084(3)	0.2497(1)	0.38817(9)	0.0035	0.5086(3)	0.2495(1)	0.38812(9)	0.0033
M3	0.4921(3)	0.8764(1)	0.0434(1)	0.0048	0.4921(3)	0.8768(1)	0.0435(1)	0.0016	0.4925(3)	0.8764(1)	0.0436(1)	0.0020
Si1	0.0730(3)	0.0664(1)	0.3896(1)	0.0042	0.0737(3)	0.0663(2)	0.3894(1)	0.0020	0.0735(3)	0.0663(2)	0.3892(1)	0.0022
Si2	0.0764(3)	0.1769(1)	0.8352(1)	0.0038	0.0758(3)	0.1767(1)	0.8350(1)	0.0027	0.0756(3)	0.1766(1)	0.8350(1)	0.0023
O1,1	0.7331(2)	0.0643(1)	0.38799(7)	0.0054	0.7338(3)	0.0642(1)	0.38791(8)	0.0031	0.7329(3)	0.0642(1)	0.38787(8)	0.0031
O1,2	0.2785(2)	0.41952(9)	0.38773(7)	0.0056	0.2782(3)	0.4193(1)	0.38780(8)	0.0034	0.2785(3)	0.4193(1)	0.38777(8)	0.0035
O1,3	0.2227(2)	0.1122(1)	0.29331(8)	0.0058	0.2231(3)	0.1122(1)	0.29322(8)	0.0033	0.2235(3)	0.1121(1)	0.29319(8)	0.0034
O1,4	0.2217(2)	0.1586(1)	0.48644(8)	0.0058	0.2222(3)	0.1586(1)	0.48660(8)	0.0036	0.2227(3)	0.1586(1)	0.48637(8)	0.0037
O2,1	0.2358(2)	0.3229(1)	0.16276(8)	0.0054	0.2347(3)	0.3228(1)	0.16275(8)	0.0031	0.2357(3)	0.3229(1)	0.16281(8)	0.0032
O2,2	0.7778(2)	0.96863(9)	0.16281(8)	0.0061	0.7771(3)	0.9689(1)	0.16261(8)	0.0034	0.7777(3)	0.9688(1)	0.16277(8)	0.0033
O2,3	0.7244(2)	0.2797(1)	0.26225(8)	0.0060	0.7251(3)	0.2797(1)	0.26241(9)	0.0036	0.7249(3)	0.2796(1)	0.26237(8)	0.0033
O2,4	0.7274(2)	0.2274(1)	0.06980(8)	0.0061	0.7285(3)	0.2270(1)	0.06971(8)	0.0035	0.7279(3)	0.2271(1)	0.06967(8)	0.0034
O/F	0.2616(3)	0.0458(1)	0.05494(8)	0.0082	0.2620(3)	0.0459(1)	0.05503(9)	0.0064	0.2613(3)	0.0461(1)	0.05508(9)	0.0060
H	0.088(1)	0.0120(6)	0.0116(4)	0.0209	0.088(1)	0.0118(6)	0.0118(5)	0.0190	0.088(1)	0.0118(6)	0.0122(5)	0.0205

TABLE 6. Atom positions and atom displacement parameters of the Tilley Foster chondrodite

	RT				100 K				10 K			
	x	*y*	*z*	U_{eq}	*x*	*y*	*z*	U_{eq}	*x*	*y*	*z*	U_{eq}
M1	1/2	0	1/2	0.0089	1/2	0	1/2	0.0060	1/2	0	1/2	0.0055
M2	0.0104(2)	0.17356(7)	0.3072(1)	0.0078	0.0102(2)	0.17377(7)	0.3069(1)	0.0054	0.0102(2)	0.17382(8)	0.3069(1)	0.0050
M3	0.4921(2)	0.88631(8)	0.0792(1)	0.0088	0.4924(2)	0.88658(8)	0.0794(1)	0.0066	0.4925(2)	0.88651(8)	0.0795(1)	0.0060
Si1	0.0760(2)	0.1442(1)	0.7040(1)	0.0067	0.0758(2)	0.1442(1)	0.7041(1)	0.0054	0.0761(2)	0.1443(1)	0.7041(1)	0.0048
O1	0.7792(2)	0.00099(7)	0.2941(1)	0.0086	0.7788(2)	0.00120(7)	0.2940(1)	0.0066	0.7789(2)	0.00113(8)	0.2939(1)	0.0061
O2	0.7268(2)	0.24079(7)	0.1251(1)	0.0087	0.7272(2)	0.24065(7)	0.1252(1)	0.0066	0.7273(2)	0.24056(8)	0.1251(1)	0.0061
O3	0.2238(2)	0.16899(7)	0.5286(1)	0.0090	0.2239(2)	0.16886(7)	0.5284(1)	0.0069	0.2241(2)	0.16887(7)	0.5284(1)	0.0063
O4	0.2646(1)	0.85471(7)	0.2946(1)	0.0086	0.2649(2)	0.85492(8)	0.2948(1)	0.0066	0.2651(2)	0.85480(8)	0.2947(1)	0.0063
O/F	0.2593(2)	0.05668(8)	0.0988(1)	0.0114	0.2590(2)	0.05679(8)	0.0987(1)	0.0086	0.2590(2)	0.05677(8)	0.0987(1)	0.0080
H	0.0895(8)	0.0138(4)	0.0190(5)	0.0269	0.0885(8)	0.0135(4)	0.0194(5)	0.0218	0.0896(8)	0.0139(4)	0.0192(5)	0.0201

TABLE 7. Refined occupancies: Mg (vs. Fe or Ti) at the M sites, F (vs. O) at the O/F sites, H at the H sites

		RT	100 K	20 K
Val Malenco titanian clinohumite				
$M1_c$	Mg	0.89(2)	0.91(2)	0.91(2)
	Fe	0.11(2)	0.09(2)	0.09(2)
$M1_n$	Mg	0.89(1)	0.89(1)	0.89(1)
	Fe	0.11(1)	0.11(1)	0.11(1)
$M2_5$	Mg	0.92(1)	0.92(2)	0.92(1)
	Fe	0.08(1)	0.08(2)	0.08(1)
$M2_6$	Mg	0.91(1)	0.91(2)	0.93(2)
	Fe	0.09(1)	0.09(2)	0.07(2)
M3	Mg	0.65(1)	0.65(2)	0.65(1)
	Fe	0.12(1)	0.13(2)	0.13(1)
	"Ti"	0.227	0.227	0.227
H		0.46(1)	0.48(2)	0.47(2)
Kukh-i-Lal clinohumite				
M3	Mg	0.896(4)	0.886(5)	0.892(5)
	Ti	0.104(4)	0.114(5)	0.108(5)
O		0.44(1)	0.52(1)	0.52(1)
H		0.40(1)	0.41(1)	0.42(1)
F		0.54(1)	0.49(1)	0.49(1)
Tilley Foster chondrodite				
M1	Mg	0.880(9)	0.89(1)	0.89(1)
	Fe	0.120(9)	0.11(1)	0.11(1)
O*		0.430(8)	0.432(8)	0.422(8)
H*		0.430(8)	0.432(8)	0.422(8)
F		0.570(8)	0.568(8)	0.578(8)

Notes: The fraction of Ti on the M3 site of the Val Malenco Ti-clinohumite has been imposed from EMA results. The sum of the occupancies was constrained to 1.
* O and H occupancies were constrained to be equal.

flight (TOF) Laue technique at the Intense Pulsed Neutron Source (IPNS) at Argonne National Laboratory. Several lattice planes were sampled in a solid volume of reciprocal space to determine the extinction conditions.

X-ray data were collected at 295 K for an equant 350 μm single crystal of the Kukh-i-Lal clinohumite on an Enraf-Nonius CAD4 four-circle diffractometer with graphite-monochromatized Mo$K\alpha$ radiation (λ = 0.71073 Å). For the refinement of the orientation matrix and unit-cell parameters 25 reflections in a 2θ range from 30.72° to 48.58° were used. A hemisphere of Bragg reflections (6067 reflections) was measured up to 2θ = 70°. The intensity loss, checked by three reflections, was 0.2% during the measurement. Intensities were corrected for Lorentz and polarization effects and the structure was refined using neutral atom scattering curves and the program SHELX97 (Sheldrick 1997). The refined atom para meters of the neutron measurement were taken as starting parameters. Details of the data collection and refinement are given in Table 11.

The longitudinal piezoelectric effect was investigated on a 4 × 4 × 1 mm plate of the Kukh-i-Lal clinohumite. A charge amplifier was used and mechanical stress was applied in different orientations. No distinct piezoelectric effect could be observed (E. Haussühl, pers. comm.).

TABLE 8. Selected octahedral and tetrahedral bond distances (Å) from RT refinements

	Val Malenco	Kukh-i-Lal		Tilley Foster
$M1_c$-O1,1 (×2)	2.096(1)	2.091(1)	M1-O1 (×2)	2.097(1)
$M1_c$-O1,2 (×2)	2.079(1)	2.072(1)	M1-O3 (×2)	2.128(1)
$M1_c$-O1,4 (×2)	2.137(1)	2.127(1)	M1-O4 (×2)	2.125(1)
< $M1_c$-O >	2.104	2.097		2.117
V (Å^3)	11.93(1)	11.818(7)		12.128(6)
OQE	1.0273(5)	1.0266(3)		1.0284(3)
$M1_n$ -O1,1	2.108(2)	2.101(2)		
$M1_n$ -O1,2	2.086(2)	2.085(2)		
$M1_n$ -O1,3	2.130(2)	2.116(1)		
$M1_n$ -O2,1	2.093(2)	2.098(2)		
$M1_n$ -O2,2	2.067(2)	2.065(2)		
$M1_n$ -O2,3	2.148(2)	2.138(2)		
< $M1_n$-O >	2.105	2.101		
V (Å^3)	11.93(1)	11.861(7)		
OQE	1.029(2)	1.024(2)		
$M2_5$ -O1,3	2.033(2)	2.028(2)	M2-O1	2.059(1)
$M2_5$-O2,1	2.176(2)	2.172(1)	M2-O2	2.235(1)
$M2_5$-O2,2	2.080(2)	2.061(1)	M2-O3	2.032(1)
$M2_5$-O2,3	2.197(2)	2.190(2)	M2-O3	2.184(1)
$M2_5$-O2,4	2.258(2)	2.221(1)	M2-O4	2.177(1)
$M2_5$ -O/F	2.059(2)	2.057(2)	M2-O/F	2.060(1)
< $M2_5$-O >	2.134	2.122		2.125
V (Å^3)	12.52(1)	12.339(8)		12.382(6)
OQE	1.0244(5)	1.0224(3)		1.0229(5)
$M2_6$ -O1,1	2.186(2)	2.181(1)		
$M2_6$-O1,2	2.059(2)	2.049(1)		
$M2_6$-O1,3	2.193(2)	2.195(1)		
$M2_6$-O1,4	2.051(2)	2.053(2)		
$M2_6$-O1,4	2.260(2)	2.236(1)		
$M2_6$-O2,3	2.074(2)	2.072(2)		
< $M2_6$-O >	2.137	2.131		
V (Å^3)	12.50(1)	12.423(8)		
OQE	1.029(1)	1.0268(9)		
M3-O2,1	2.116(2)	2.112(2)	M3-O1	2.192(1)
M3-O2,2	2.204(2)	2.191(2)	M3-O2	2.001(1)
M3-O2,4	2.115(2)	2.106(2)	M3-O2	2.121(1)
M3-O2,4	1.985(2)	1.995(2)	M3-O4	2.124(1)
M3-O/F	2.035(2)	2.030(2)	M3-O/F	2.033(1)
M3-O/F	2.070(2)	2.050(2)	M3-O/F	2.059(1)
<M3-O>	2.088	2.081		2.088
V (Å^3)	11.81(1)	11.704(8)		11.849(5)
OQE	1.019(2)	1.018(2)		1.018(1)
Si1-O1,1	1.609(2)	1.612(2)	Si1-O1	1.647(1)
Si1-O1,2	1.652(2)	1.656(2)	Si1-O2	1.638(1)
Si1-O1,3	1.638(2)	1.638(2)	Si1-O3	1.643(1)
Si1-O1,4	1.634(2)	1.632(2)	Si1-O4	1.614(1)
<Si1-O>	1.633	1.635		1.636
V (Å^3)	2.203(3)	2.205(2)		2.212(2)
TQE	1.010(1)	1.011(1)		1.0099(9)
Si2-O2,1	1.611(2)	1.615(2)		
Si2-O2,2	1.644(2)	1.647(1)		
Si2-O2,3	1.635(2)	1.638(2)		
Si2-O2,4	1.640(2)	1.636(2)		
<Si2-O>	1.633	1.634		
V (Å^3)	2.200(3)	2.203(2)		
TQE	1.010(2)	1.011(2)		

Note: The octahedral (OQE) and tetrahedral (TQE) quadratic elongation is given after Robinson et al. (1971).

RESULTS AND DISCUSSION

Our results confirm that within standard deviations all Ti is concentrated in the M3 site of the Kukh-i-Lal clinohumite (Fujino and Takéuchi 1978). For the Val Malenco clinohumite the Ti-content derived from the EMA measurement was fixed on the M3 site. Gibbs et al. (1970) found that Fe preferred the M1 position in chondrodite, the only site with no (F, OH) ligands. Refinement of the Tilley Foster chondrodite also revealed that Fe exclusively occupies the M1 site (~10%). The H position of the F-bearing chondrodite corresponds to the D1 position of deuterated hydroxylchondrodite (Lager et al. 2001).

Abbott et al. (1989) have used structure energy calculations to locate the H atom in several humite minerals, including hydroxylchondrodite, titanian chondrodite and titanian clinohumite. The locations of energy minima for H^+ were consistent with the two types of H sites, as determined in the studies by Yamamoto (1977) and Fujino and Takéuchi (1978). The effect of the substitutions $F(OH)_{-1}$ and $TiO_2M_{-1}(OH)_{-2}$ on the location of the minima was also investigated. The major conclusions were that H1 sites were only found when adjacent anion sites were occupied by OH, and that H2 sites were favored when either Ti or F was included in the local environment. Both of these conclusions are in disagreement with the refinement of Fujino and Takéuchi (1978), and with the results of this study, where only H1-type sites in titanian clinohumite are observed. With the exception of the *x*-coordinate, the experimentally determined H position is in good agreement with that determined by Abbott et al. (1989) for the H1 site.

TABLE 11. Details on X-ray data collection and refinement of the Kukh-i-Lal clinohumite

a (Å)	4.7381(5)
b (Å)	10.2379(6)
c (Å)	13.647(1)
α (°)	100.899(6)
V (Å^3)	650.02(9)
ρ_{calc} (g/cm^3)	3.116
μ(Mo*K*α) (mm^{-1})	1.12
Extinction coefficient	6.0×10^{-2}
$2\theta_{max}$ (°)	70
Reflections measured	6067
Unique reflections	2858
No. Variables	151
Goof	1.209
R (all)	0.0232
wR^2 (on F^2)	0.0591
$\Delta\rho_{max/min}$ (e$^-$/Å^3)	0.56/-0.58

Notes:
$R = \Sigma||F_o| - |F_c| / S\,|F_o||$.
$wR^2 = [\Sigma\, w(F_o^2 - F_c^2)^2 / \Sigma\, wF_o^4]^{1/2}$.

TABLE 9. Selected interatomic distances (Å) and angles (°) related to the OH, F substitution and angles to the OH,F substitution

	Val Malenco			Kukh-i-Lal			Tilley Foster		
	RT	100 K	20 K	RT	100 K	20 K	RT	100 K	10 K
O-H	1.029(6)	1.029(7)	1.021(7)	1.034(6)	1.034(6)	1.029(6)	1.028(4)	1.028(4)	1.024(4)
O/F-O/F	2.898(2)	2.889(3)	2.891(3)	2.958(2)	2.960(2)	2.956(2)	2.939(1)	2.934(1)	2.932(1)
H···O/F	1.872(6)	1.863(7)	1.873(7)	1.929(6)	1.930(6)	1.931(6)	1.918(4)	1.912(4)	1.916(4)
O-H···O/F	174.6(5)	173.9(6)	174.2(6)	173.2(5)	173.4(6)	173.6(6)	171.7(3)	172.1(3)	171.8(3)
O/F-O2,2/O1	2.957(2)	2.948(2)	2.948(2)	2.954(2)	2.949(2)	2.951(2)	2.962(1)	2.957(1)	2.954(1)
H···O2,2/O1	2.536(6)	2.525(7)	2.525(7)	2.508(5)	2.506(7)	2.513(7)	2.502(4)	2.502(4)	2.496(4)
O-H···O2,2/O1	103.9(4)	104.0(5)	104.2(5)	105.3(4)	105.0(4)	105.0(4)	106.5(3)	106.1(2)	106.5(3)
H-H	0.853(8)	0.85(1)	0.86(1)	0.91(1)	0.91(1)	0.92(1)	0.913(7)	0.904(7)	0.915(7)

Structural variations on Ti and F substitution

The O-H distances vary within one standard deviation in a range of 1.028(4) to 1.034(6) Å at ambient temperature. These distances are relatively long if compared to the mean value of 0.969(1) Å determined by Ceccarelli et al. (1981) from neutron diffraction data. The difference can be attributed to the statistically varying function of the O/F atom both as donor and as acceptor that derives from a disordered distribution of the centrosymmetrically related H atoms (Fig. 2). The different positions of the O and F atoms are also in our case reflected by the elongated atomic displacement ellipsoid. The unusually long O-D bonds in synthetic deuterated hydroxylchondrodite [O-D1 = 1.076(4) Å; O-D2 = 1.110(4) Å] have also been related to the positional disorder of the O atom (Lager et al. 2001).

There is one strong and one weak H bond in both the clinohumites and F-bearing chondrodite (Table 9). For the strong H bond, O/F-O/F distances range from 2.898(2) to 2.939(1) Å with angles of 174.6(5)° to 171.7(3)°. In the clinohumites, the weak H bond is characterized by O/F-O2,2 distances of 2.957(2) and 2.954(2) Å and angles of 103.9(4) and 105.3(4)°, respectively. In the chondrodite, the weak H bond has an O/F-O1 distance of 2.962(1) Å with an angle of 106.5(3)°.

The refined occupancies of the H site are 47(2)%, 42(1)%, and 40(2)%, respectively, for the Val Malenco clinohumite, the F-bearing Tilley Foster chondrodite and the F-bearing Kukh-i-Lal clinohumite. It has been proposed that natural samples avoid occupancies greater than 50% (Yamamoto 1977; Ribbe 1982; Fujino and Takéuchi 1978). The $TiO_2M_{-1}(OH)_{-2}$ substitution maintains charge balance and stabilizes the crystal structure avoiding steric hindrance between the two H atoms. If the occupancy of the H site exceeds 50%, distances between centrosymmetric pairs of H atoms would range from 0.853 to 0.916 Å (Table 9) for the structures refined in this study, leading to proton-proton repulsion. H occupancies less than 50% are possible as long as the geochemical environment provides sufficient F and/or Ti. Trace amounts of these ions or their complete absence during formation requires H occupations above 50% (OH > 1 atoms per formula unit), which, in turn, leads to two H sites in order to avoid short H-H distances (Yamamoto 1977; Ferraris et al. 2000; Lager et al. 2001; Berry and James 2001). This suggests that the rare occurrence of nearly stoichiometric hydroxylclinohumite and hydroxylchondrodite in nature is related to compositional rather than crystal-chemical constraints (Berry and James 2001).

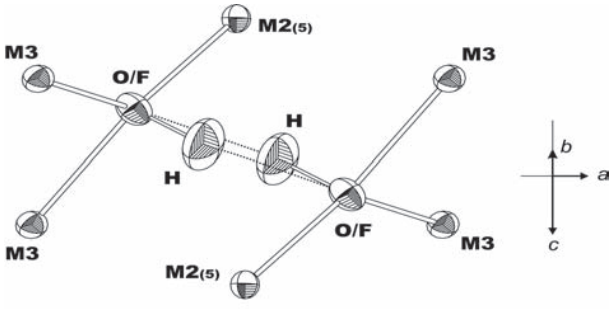

FIGURE 2. The O-H bond geometry of the natural clinohumite and chondrodite samples using the Tilley Foster chondrodite as an example. Displacement ellipsoids are drawn with a scale factor of 2.

The $F(OH)_{-1}$-substitution at the O/F-site does not significantly affect intra-polyhedral bond distances and angles of clinohumites, except for one M3-O/F bond that decreases from 2.070(2) Å in the F-free Val Malenco clinohumite to a distance of 2.050(2) Å in the F-bearing Kukh-i-Lal clinohumite. The change in this bond distance is accompanied by an increase of one of the two inter-polyhedral $M2_5$-O/F-M3 angles from 128.74(10)° to 129.85(7)°. The shorter M3-O bond distance in F-bearing clinohumite is not what one would expect based on the larger octahedral cation radius of Mg^{2+}. In order to maintain charge balance, the $Ti^{4+} \leftrightarrow Mg^{2+}$ substitution locally occurs concomitant with $O^{2-} \leftrightarrow OH$ substitution. The negative coupling of the Ti^{4+} content to the OH concentration also causes a negative correlation between Ti^{4+} and F^-. Therefore, the size-effect due to the $Ti^{4+} \leftrightarrow Mg^{2+}$ substitution [ionic radii (IR) = 0.605 Å and 0.72 Å, respectively] can be counterbalanced by the opposed effect of the $O^{2-} \leftrightarrow OH$ (IR = 1.36 and 1.34, respectively) as well as the $OH \leftrightarrow F$ (IR = 1.34 and 1.30) substitution.

The O/F-O/F distance [2.958(2) Å] of F-bearing clinohumite is slightly longer than that of the F-free sample [2.898(2) Å], despite the nominally smaller ionic radius of F relative to OH. In F-bearing clinohumite, the H···O/F distance is longer and the O-H···O/F angle narrower, even though the O-H bond lengths for the two clinohumites are equivalent within experimental error. One would expect shorter H bonds in F-bearing clinohumite because F^- is a stronger hydrogen bond acceptor than O^{2-}. These seemingly anomalous variations can be interpreted in terms of the occupancy of the H site, which is negatively correlated to the Ti-content (see above). The split H site of the F-bearing clinohumite has a lower occupancy (41% vs. 47%), which leads to a reduced number of H bonds in this structure (82%) compared to F-free clinohumite (94%). Vacant H positions result in anion-anion repulsion, which increases the mean O/F-O/F length. On the other hand, occupation of a H site results in an additional cation-cation repulsion between H and the M3 metals (Fig. 1). These two effects combine to produce a shearing of the M3-O/F-M3-O/F quadrilateral (Fig. 1) with increasing F content (= decreasing H-occupation), making it more regular at high F-content. The coordination of the O/F atom becomes less pyramidal and more planar. The sum of the three M-O/F-M angles changes from 352.75° to 354.21°, which corresponds to a reduction of the acceptor/donor function of the O/F atom.

Comparison of our neutron data with the X-ray data collected by Weiss (1997) for a clinohumite (CH-13) of similar composition shows some significant differences in the M3-O bond distances (e.g., M3-O2,1 = 2.194 Å, M3-O2,4 = 2.173 Å, M3-O/F = 1.980 and 1.988 Å in CH-13; Table 8). This difference could be due to the large relative difference in the neutron scattering lengths of Mg and Ti, making our neutron data more sensitive to the M3 atom position when compared to X-ray data.

The observed differences in individual bond lengths are also reflected in the unit-cell parameters and volume (Table 2), as previously observed by Ribbe (1979). In F-free titanian

clinohumite and titanian chondrodite, Fujino and Takéuchi (1978) noticed a slight increase in cell parameters, especially in the *b* axis, with increasing Ti content. Since the M3-O/F bond is oriented almost parallel to the *b* axis, the preferred expansion of the *b* axis supports this hypothesis. If one compares intra-polyhedral bond distances and polyhedral volumes (Table 8) of the Kukh-i-Lal and the Val Malenco clinohumite, as well as the quadratic elongations of the polyhedra, it is evident that most coordination polyhedra do not contribute significantly to the difference in molar volume. Only the $M2_5$-O_6 polyhedron shows a relevant volume difference. In particular, the $M2_5$-O2,2 bond length increases with decreasing F and increasing Ti content from 2.061(1) Å for the Kukh-i-Lal clinohumite to 2.080(2) Å for the Val Malenco titanian clinohumite. This can be explained by the fact that local Ti^{4+} occupation on M3 leads to a stronger M3-O2,2 bond. This weakens and thus lengthens the $M2_5$-O2,2 bond. Since this bond, like the M3-O/F bond, lies nearly parallel to the *b* axis if projected in the (100) plane, the *b* axis will be most affected by an increase in Ti concentration (Table 2). Only a few of the intra-polyhedral and inter-polyhedral angles are significantly different (up to 1.81°, Table 12) between the two clinohumite structures; most of the angles remain constant within 0.6°. It is not surprising that the angles which are most sensitive to the OH/F ratio are associated with the M3 and the $M2_5$ octahedra.

Space-group violations

As described above, a random but mutually exclusive distribution of the H atoms at the centrosymmetrically related positions has to be assumed due to H-H repulsion. It is possible that the H atoms could become ordered at lower temperatures leading to a reduction in space-group symmetry. We did observe a few weak [with a maximum of $F \leq 6\ \sigma(F)$] reflections that violated the space-group symmetry. These were present at each temperature and mainly affected the *b*-glide plane [$0kl$: $k = 2n + 1$] and, to a lesser extent, the 2_1 screw axis [$h00$: $h = 2n + 1$]. However, the "forbidden" reflections were not the same in all the samples and no new violations were observed at lower temperatures. Furthermore, the intensity of these reflections was essentially independent of temperature. Single-crystal TOF data of the Val Malenco titanian clinohumite at 295 and 20 K, and X-ray single-crystal data of the Kukh-i-Lal clinohumite at 295 K confirmed the presence of the same symmetry-forbidden reflections observed in the equivalent single-crystal neutron data set on the HB2a diffractometer at ORNL. Thus it seems unlikely that they are due to H ordering alone. As only a few weak peaks are present in each data set, the refinement in space group $P2_1/b$ is justified. Refinement of the X-ray structure in space-group $P2_1$ was attempted but did not improve the *R* values of the fit, despite a significant increase in the number of refineable parameters. The observed differences in bond-lengths between $P2_1$ and $P2_1/b$ were also within the expected range and did not support a non-centrosymmetric model. In addition, piezoelectric measurements of the Kukh-i-Lal clinohumite did not show any indication of a piezoelectric effect. The interpretation that the space-group violations are due to Renninger Umweg effects was excluded because the Bragg intensity was constant with varying psi angle. The most probable interpretation is local ordering of H, and possibly Ti, which might account for the observed reflections as suggested by Smyth et al. (1994). As pointed out above, both centrosymmetrically related H positions cannot be simultaneously occupied because of H-H repulsion. This means that the center of symmetry is locally violated by H atoms. Ordering would give rise to enantiomorphic domains of local symmetry $P2_1$ and *Pb*, the coexistence of which would eliminate any observable piezoelectric effect. A larger domain size in the Kukh-i-Lal gem-quality specimen would account for the stronger reflections observed.

TABLE 12. Selected intra-polyhedral and inter-polyhedral angles (°) in clinohumites displaying the greatest differences (Δ)

	Val Malenco	Δ (°)	Kukh-i-Lal
O1,3-$M2_5$-O/F	104.99(8)	1.81	103.18(7)
M3-O2,4-Si2	123.8(1)	1.32	122.52(8)
$M2_5$-O/F-M3	128.7(1)	–1.11	129.85(7)
O2,2-M3-O2,4	171.0(1)	–1.04	172.01(8)
O1,4-$M2_6$-O2,3	110.45(9)	0.97	109.48(7)
O2,3-$M2_5$-O/F	162.57(8)	–0.85	163.42(7)
O2,4-$M2_5$-O/F	92.95(7)	–0.84	93.79(6)
O2,2-M3-O/F	92.75(9)	0.83	91.92(7)

ACKNOWLEDGMENTS

Oak Ridge National Laboratory is managed by UT-Battelle, LLC, for the U.S. Department of Energy under contract DE-AC05-00OR22725. Argonne National Laboratory is supported by the U.S. Department of Energy, Basic Energy Sciences under contract W-31-109-ENG-38 with the University of Chicago. A. Friedrich was financially supported by the Swiss National Science Foundation (Credit 21-052682.97 to M. Kunz). G. Lager acknowledges support from the National Science Foundation through grant EAR-0073734. Thanks are due to M. Weiss and P. Ulmer for making available the Val Malenco clinohumite crystal. The authors thank E. Reusser, A. Buob, and P. Ulmer for their support in handling the electron microprobe analyses of the clinohumites. We thank E. Haussühl for carrying out the piezoelectric measurement and L.A. Groat for the electron microprobe analysis of the Tilley Foster chondrodite. Constructive reviews by F. Camara, N. Ross, and R. Oberti significantly improved the manuscript.

REFERENCES CITED

Abbott Jr., R.N., Burnham, C.W., and Post, J.E. (1989) Hydrogen in humite-group minerals: Structure-energy calculations. American Mineralogist, 74, 1300–1306.

Akaogi, M. and Akimoto, S.-I. (1980) High-pressure stability of a dense hydrous magnesian silicate $Mg_{23}Si_8O_{42}H_6$ and some geophysical implications. Journal of Geophysical Research, 85, B12, 6944–6948.

———(1986) Infrared spectra of high-pressure hydrous silicates in the system MgO-SiO_2-H_2O. Physics and Chemistry of Minerals, 13, 161–164.

Berry, A.J. and James, M. (2001) Refinement of hydrogen positions in synthetic hydroxylclinohumite by powder neutron diffraction. American Mineralogist, 86, 181–184.

Cámara, F. (1997) New data on the structure of norbergite: location of hydrogen by X-ray diffraction. Canadian Mineralogist, 35, 1523–1530.

Ceccarelli, C., Jeffrey, G.A., and Taylor, R. (1981) A survey of O-H...O hydrogen bond geometries determined by neutron diffraction. Journal of Molecular Structure, 70, 255–271.

Cynn, H., Hofmeister, A.M., Burnley, P.C., and Navrotsky, A. (1996) Thermodynamic properties and hydrogen speciation from vibrational spectra of dense hydrous magnesium silicates. Physics and Chemistry of Minerals, 23, 361–376.

Faust, J. and Knittle, E. (1994) Static compression of chondrodite: Implications for water in the upper mantle. Geophysical Research Letters, 21, 1935–1938.

Ferraris, G., Prencipe, M., Sokolova, E.V., Gekimyants, V.M., and Spiridonov, E.M. (2000) Hydroxylclinohumite, a new member of the humite group: Twinning, crystal structure and crystal chemistry of the clinohumite subgroup. Zeitschrift für Kristallographie, 215, 169–173.

Friedrich, A., Kunz, M., Miletich, R., and Lager, G.A. (2000) Compressibility of chondrodite, $Mg_5(SiO_4)_2(OH,F)_2$ up to 9.6 GPa: The effect of F/OH substitution on the bulk modulus. Journal of Conference Abstracts, 5, 37.

Fritzel, T.L.B. and Bass, J.D. (1997) Sound velocities of clinohumite, and implications for water in Earth's upper mantle. Geophysical Research Letters, 24, 1023–1026.

Fujino, K. and Takéuchi, Y. (1978) Crystal chemistry of titanian chondrodite and titanian clinohumite of high-pressure origin. American Mineralogist, 63, 535–543.
Gibbs, G.V. and Ribbe, P.H. (1969) The crystal structures of the humite minerals: I. Norbergite. American Mineralogist, 54, 376–390.
Gibbs, G.V., Ribbe, P.H., and Anderson, C.P. (1970) The crystal structures of the humite minerals: II. Chondrodite. American Mineralogist, 55, 1182–1195.
Jones, N.W. (1969) Crystallographic nomenclature and twinning in the humite minerals. American Mineralogist, 54, 309–313.
Jones, N.W., Ribbe, P.H., and Gibbs, G.V. (1969) Crystal chemistry of the humite minerals. American Mineralogist, 54, 391–411.
Kocman, V. and Rucklidge, J. (1973) The crystal structure of titaniferous clinohumite. Canadian Mineralogist, 12, 39–45.
Kuribayashi, T., Kudoh, Y., and Akizuki, M. (1998) Single-crystal X-ray diffraction and FTIR spectra of chondrodite, $Mg_5Si_2O_8(OH,F)_2$ under high pressure to 6.0 GPa. 17th General Meeting of the International Mineralogical Association, Toronto, A44.
Lager, G.A., Ulmer, P., Miletich, R., and Marshall, W.G. (1999) Crystal structure and static compression of OD-chondrodite. EOS, Transactions of the American Geophysical Union, 80, F1139.
Lager, G.A., Ulmer, P., Miletich, R., and Marshall, W.G. (2001) O-D···O bond geometry in OD-chondrodite. American Mineralogist, 86, 176–180.
Larson, A.C. and Von Dreele, R.B. (1994) General Structure Analysis System. Los Alamos National Laboratory Report LAUR 86–748.
Lin, C.-C., Liu, L.-G., and Irifune, T. (1999) High-pressure Raman spectroscopic study of chondrodite. Physics and Chemistry of Minerals, 26, 226–233.
Lin, C.-C., Liu, L.-G., Mernagh, T.P., and Irifune, T. (2000) Raman spectroscopic study of hydroxyl-clinohumite at various pressures and temperatures. Physics and Chemistry of Minerals, 27, 320–331.
Mernagh, T.P., Liu, L.G., and Lin, C.C. (1999) Raman spectra of chondrodite at various temperatures. Journal of Raman Spectroscopy, 30, 963–969.
Phillips, B.L., Burnley, P.C., Worminghaus, K., and Navrotsky, A. (1997) ^{29}Si and ^{1}H NMR spectroscopy of high-pressure hydrous magnesium silicates. Physics and Chemistry of Minerals, 24, 179–190.
Ribbe, P.H. (1979) Titanium, fluorine, and hydroxyl in the humite minerals. American Mineralogist, 64, 1027–1035.
———(1982) The humite series and Mn-analogs. In P.H. Ribbe, Ed., Mineralogial Society of America Reviews in Mineralogy, 5, 231–274.
Ribbe, P.H. and Gibbs, G.V. (1971) Crystal structures of the humite minerals: III. Mg/Fe ordering in humite and its relation to other ferromagnesian silicates. American Mineralogist, 56, 1155–1173.
Ribbe, P.H., Gibbs, G.V., and Jones, N.W. (1968) Cation and anion substitutions in the humite minerals. Mineralogical Magazine, 37, 966–975.
Robinson, K., Gibbs, G.V., and Ribbe, P.H. (1971) Quadratic elongation: A quantitative measure of distortion in coordinaton polyhedra. Science, 172, 567–570.
———(1973) The crystal structures of the humite minerals. IV. Clinohumite and Titanoclinohumite. American Mineralogist, 58, 43–49.
Ross, N.L. and Crichton, W.A. (2000) Compression of hydroxyl-clinohumite ($Mg_9Si_4O_{16}(OH)_2$) and hydroxyl-chondrodite ($Mg_5Si_2O_8(OH)_2$). American Mineralogist, in press.
Sheldrick, G.M. (1997) SHELXL-97 and SHELXS-97. Programs for crystal structure determination. University of Göttingen, Germany.
Sinogeikin, S.V. and Bass, J.D. (1999) Single-crystal elastic properties of chondrodite: Implications for water in the upper mantle. Physics and Chemistry of Minerals, 26, 297–303.
Smyth, J.R., Swope, R.J., and Larson, A.C. (1994) Crystal chemistry of H in clinohumite. EOS, Transactions of the American Geophysical Union, 75, supplement 1, 231–232.
Thompson, A.B. (1992) Water in the Earth's upper mantle. Nature, 358, 295–302.
Weiss, M. (1997) Clinohumite: A field and experimental study. A dissertation of the Swiss Federal Institute of Technology Zürich (ETH), Diss. ETH No. 12202.
Williams, Q. (1992) A vibrational spectroscopic study of hydrogen in high pressure mineral assemblages. In Y. Syono and M.H. Manghnani, Eds., High-Pressure Research: Application to Earth and Planetary Sciences, Terra Publishing Company, 289–296.
Yamamoto, K. (1977) The crystal structure of hydroxyl-chondrodite. Acta Crystallographica, B33, 1481–1485.
Yamamoto, K. and Akimoto, S.-I. (1977) The system MgO-SiO_2-H_2O at high pressures and temperatures–stability field for hydroxyl-chondrodite, hydroxyl-clinohumite and 10 Å phase. American Journal of Science, 277, 288–312.

MANUSCRIPT RECEIVED AUGUST 28, 2000
MANUSCRIPT ACCEPTED MAY 19, 2001
PAPER HANDLED BY ROBERTA OBERTI